Taylor dispersion analysis discloses the impairment of Aβ peptide aggregation by the presence of a fluorescent tag

Mihai Deleanu, Jean-François Hernandez, Hervé Cottet, Joseph Chamieh

Taylor dispersion analysis discloses the impairment of Aβ peptide aggregation by the presence of a fluorescent tag

Mihai Deleanu[1], Jean-François Hernandez[1], Hervé Cottet[*1], Joseph Chamieh*[*1]*

[1]IBMM, Université Montpellier, CNRS, ENSCM, Montpellier, France

Abstract

The use of fluorescently tagged amyloid peptides, implicated in Alzheimer's disease, to study their aggregation at low concentrations is a common method, however the fluorescent tag should not introduce a bias in the aggregation process. In this work, native amyloid peptides Aβ(1-40) and Aβ(1-42) and Fluorescein-5-isothiocyanate (FITC) tagged ones, were studied using Taylor dispersion analysis (TDA) coupled with a simultaneous UV and Light Emmitting Diode Induced Fluorescence (LEDIF) detection, to unravel the effect of FITC on the aggregation process. For that, a total concentration of 100 μM of peptides consisting of a mixture of native and tagged ones (up to 10% in moles), was applied. Results demonstrated that FITC had a strong inhibition effect upon the aggregation behavior of Aβ(1-42), while for Aβ(1-40), only a retardation in kinetics was observed. It was also shown that when mixed solutions of Aβ(1-40) and Aβ(1-42) are used, the Aβ(1-42) alloform was the leading peptide in the aggregation process, and when the latter was tagged the aggregation kinetics decreased but the lifetime of potentially toxic oligomers was drastically increased. These results confirmed, that the hydrophilicity of the *N*-terminus part of the peptide plays a major role in the aggregation process.

1. Introduction

Alzheimer's disease (AD) is a neurodegenerative pathology inducing damage to the patient's brain and translating in memory loss and behavioural impairment. One of the main hallmarks of AD is the presence of amyloid β peptide (Aβ) plaques in the brain of patients and several evidence points that Aβ peptides are one of the main reasons behind the symptoms of AD either in its oligomeric form (thought to be neurotoxic)[1, 2] or in its fibrillary form[3].

In all cases, there is a necessity to better understand the aggregation mechanism of Aβ peptides. However *in vitro* studies are often hampered by the detection limits of the used methods which often impose the use of concentrations (μM range) several tens of times higher than the *in vivo* ones (nM range[4]). Studying the aggregation process of amyloid peptides in detail is a challenging task especially at concentrations in the order of magnitude of physiological ones. For that, the use of selective and sensitive detection methods such as fluorescence based ones is highly desirable to study peptides at lower concentrations[5]. This strategy implies a modification of the peptide structure by adding a label often on its *N*-terminal end. However, the attached tag may affect the physical and chemical properties of the amyloid peptides[6] and their propensity to form beta-sheets and thus fibrillar structures. Wägele *et al.*[6] studied by fluorescence correlation spectroscopy (FCS) the effect of four fluorescent tags (HLyte 647, HiLyte 488, Atto 655 and Atto 488) on the oligomer distribution of both Aβ(1-40) and Aβ(1-42). They concluded that HiLyte 647 and Atto 655, compared to the other two tags, had high peptide-tag interactions which promoted the formation of the high molecular weight oligomers of Aβ(1-40) and consequently the fibrillation step. In this experiment, Atto 488 seemed to be the most suitable as no significant interaction was noted. Quinn *et al.* [7] demonstrated that HiLyte fluor 555-labelling of Aβ peptides on its *N*-terminus did not alter the self-assembly kinetics or the resulting aggregated structures. On the contrary, Taverna *et al.* demonstrated that a fluorescent tag (Fluoprobe 488 NHS Ester) attached on a side-chain of amyloid Aβ(1-42) (on the amines of Lys-16, Lys-28 and/or *N*-terminus Asp residues) inhibited the aggregation [8]. In another study by Zheng *et al*. [9], the effect of five different dyes introduced in the form of *N*-hydroxysuccinimidyl esters (BP, RB and 5-SFX) or as isothiocyanates (RITC and 5-(6)-FITC) was evaluated. The authors concluded that 5-SFX and 5-(6)-FITC inhibited the aggregation, since no change in the R_h was observed during the incubation period of 4 h, while the other three promoted it. However, this study showed limitations as a concentration

of 5 µM in peptide was used and the aggregation was monitored for only few hours at 25 °C. Under these conditions the aggregation of the Aβ peptides would take a few days (even weeks)[10] to start and it seems difficult to judge on the inhibition effect of these dyes. In our opinion, in order to study the aggregation process of amyloid peptides at relevant physiological concentrations one might consider the use of preformed seeds known to accelerate the aggregation process at such low concentrations [11]. Eventhough, when labelled peptides are used, it is important to understand if the attached label is not introducing a bias in the aggregation process.

Amyloid peptides exist under different isoforms, the most common ones being Aβ(1-40) and Aβ(1-42), which differ from the former by two extra amino acids at the C-terminus, making it more hydrophobic. These co-existing isoforms aggregate differently when separate[12, 13]. However, *in vivo* these isoforms coexist and it is not clear how they influence each other. In fact, it was found that the amyloid plaques in the brains of AD patients were mainly, and sometimes exclusively, constituted of Aβ(1-42)[14], despite that Aβ(1-40) concentration is several-fold higher than Aβ(1-42) one. The co-aggregation of these two isoforms was intensively studied over the last decade[15, 16]. Some authors claimed that the peptide mixing only influences the elongation phase by seeding the fibrillation but no heteromolecular fibrils are formed[16]. But other reports suggested that mixed fibrils could be formed[15, 17].

In previous works, we showed the potential of Taylor dispersion analysis (TDA) to speciate the aggregation process of Aβ(1-40) and Aβ(1-42), as pure or mixed peptide solutions[13, 18]. In this work we present the use of TDA coupled with simultaneous UV and LEDIF detections to study the influence of the fluorescent tag FITC on the Aβ peptide aggregation and to unravel if heteromolecular species are formed along the aggregation course.

2. Materials and methods

2.1. Materials

Aβ(1–40) was prepared by fast conventional SPPS using a *Fmoc* orthogonal strategy, as described elsewhere[13]. Aβ(1-42) (batch number 100002591, >95% purity by HPLC), were purchased from Bachem (Bubendorf, Switzerland). Both FITC peptides were tagged on their *N*-terminal side, and the molar mass of the tagged peptides was confirmed by MALDI-MS (provider) and HPLC-ESI-MS in this work (4790 g/mol and 5016 g/mol for tagged Aβ(1-40)

and tagged Aβ(1-42) respectively). Sodium dihydrogeno phosphate and sodium hydroxide were purchased from Sigma Aldrich (France). All buffers were prepared using ultrapure water obtained from a MilliQ system (Millipore, France).

2.2. Peptide pretreatment and sample preparation

Both native (nAβ) and tagged (tAβ) peptides were pretreated independently using the protocol previously described[13, 19]. Briefly, the peptides were first dissolved at a concentration of 2 g/L in an ammonium hydroxide solution (NH_4OH) which concentration differed between the two studied peptides (0.10 % (m/v) for Aβ(1-40), 0.16 % (m/v) for Aβ(1-42)). The peptide solutions were then incubated for 10 minutes at room temperature, then aliquoted and freeze-dried. The stock aliquots contained 10 nmol of peptide, and lyophilized peptide aliquots were stored at -20 °C until use. The pure tagged or native peptide solutions were prepared directly from the aliquoted fractions and dissolved in the adequate amount of buffer to reach the desired final peptide concentrations of 1, 10 and 100 µM.

The mixed aliquots containing both native and tagged Aβ were prepared so that the final sample contained either 7% of tAβ(1-40) or 10% of tAβ(1-42). First stock aliquot of native or tagged peptides was dissolved in 100 µL of 0.16% (m/v) NH_4OH, then appropriate volumes were used to obtain the desired combinations having a total Aβ content of 10 nmol, as detailed in table 1. Figures 1, 2 and 5 show pie charts with the proportion of the native and tagged peptides in the samples. The final aliquots were immediately subjected to freeze-drying and then stored at -20°C before being dissolved in 20 mM phosphate buffer at pH 7.4 to perform the aggregation study.

Table 1: Peptide quantities (nmol) and proportions in the mixed native/tagged samples

	Peptide quantities (nmol) and (proportions)			
Sample	**nAβ(1-40)**	**nAβ(1-42)**	**tAβ(1-40)**	**tAβ(1-42)**
Aβ(1-40) with tAβ(1-40)	9.3 (93 %)		0.7 (7 %)	
Aβ(1-42) with tAβ(1-42)		9 (90 %)		1 (10 %)
3:1 Aβ(1-40):Aβ(1-42)	7.5 (75 %)	2.5 (25 %)		
3:1 Aβ(1-40):Aβ(1-42) with tAβ(1-40)	6.8 (68 %)	2.5 (25 %)	0.7 (7 %)	
3:1 Aβ(1-40):Aβ(1-42) with tAβ(1-42)	7.5 (75 %)	1.5 (15 %)		1 (10 %)

2.3. Study of Aβ aggregation by Taylor dispersion analysis

TDA was performed using an Agilent 7100 (Waldbronn, Germany) capillary electrophoresis system with bare fused silica capillary (Polymicro technologies, USA), having 60 cm × 50 µm i.d. dimensions and a UV detection window at 51.5 cm from the inlet end. The system was coupled with a Zetalif light-emitting diode induced fluorescence (LEDIF) detector (Picometrics, Toulouse, France) with a window at 33 cm from the inlet end. The capillary was conditioned with the following flushes: 1 M NaOH (30 min) followed by a flush with ultrapure water (30 min). Between each analysis, the capillary was rinsed with a 20 mM sodium phosphate buffer at pH 7.4 for 2 min. Samples were injected hydrodynamically on the inlet end of the capillary (44 mbar, 4 s) and the injected volume was about 6.5 nL, corresponding to 1% of the capillary volume to the LEDIF detection point and 0.64% with respect to the UV detection window. In the case of the 1µM, 10 µM and 100 µM tAβ(1-42) samples, the solutions were injected hydrodynamically by applying for 3 s a pressure of 33, 55 and 6 mbar respectively. The injection volumes were modified to prevent detector saturation.

Experiments were performed at a mobilization pressure of 100 mbar. The temperature of the capillary cartridge was set at 37 °C and the vial carrousel was thermostated using an external circulating water bath 600F from Julabo (Germany). The solutes were simultaneously monitored by UV with an absorbance measured at 191 nm and by fluorescence with an excitation at 480 nm. Emission light was collected through a ball lens and a high-pass filter in the wavelength range from 515–760 nm. The proportion of tagged peptide in the mixtures was chosen so that the obtained LEDIF signal was as high as possible without saturating the detector. The higher fluorescence intensity observed for tAβ(1-40) presumably stems from the presence of unreacted FITC during synthesis, as observed for these samples from the taylorgrams (see supporting information Figures SI.1 to SI.8). The mobile phase was a 20 mM sodium phosphate buffer (pH 7.4; viscosity at 37 °C: 0.7×10^{-4} Pa.s). Peptide aliquots were first dissolved in 100 µL of a 20 mM sodium phosphate buffer solution (pH 7.4) to reach a final concentration of 100 µM and then immediately transferred to a vial to be incubated at 37°C in the capillary electrophoresis carrousel. The aggregation was conducted by injecting the sample ($V_{inj} \approx 7$ nL) every 11 min for 100% Aβ(1-42) experiments, and each 30 min for all the experiments containing Aβ(1-40). The total average of TDA injections was between 124 and 185 TDA runs per sample, corresponding to a total sample volume consumption between 870 to 1300 nL (0.87 and 1.3 µL). Finally, to prevent sample evaporation, the vial cap was changed three times a day. All taylorgrams were recorded using Agilent Chemstation software and then

exported to Microsoft Excel for subsequent data processing. The data obtained from the UV signal were treated on the right side of the taylorgram to avoid the spikes detected on the left part, as described elsewhere[13, 18].

3. Results and discussion

3.1. Influence of the peptide concentration

The effect of the peptide concentration on the kinetics of the aggregation process was first investigated by TDA at different tagged peptide (tAβ(1-42)) concentrations ranging from 1 to 100 µM. As can be seen from Figure 1A, the total peak area, obtained by integrating the taylorgrams from the LEDIF detection, did not evolve significantly in the case of the lowest concentrations (1 and 10 µM), over the whole studied incubation time (352 h for the 1µM sample and 162 h for the 10 µM sample), suggesting that the kinetics of the aggregation at these concentrations is very slow, as shown in the literature the kinetics of the aggregation increase with increasing concentration[20]. The normalization of the peak area in Figure 1A was realized for the sake of comparison and was obtained by dividing each peak area of each run by the peak area obtained at t_{ag} = 0 h.

In the case of the highest concentration (*i.e.* 100 µM), the peak area decreased to reach a plateau after ~3 h of incubation. The comparison with a sample having the same 100 µM total peptide concentration but with a mixing of 90 µM nAβ(1-42) with 10 µM of tAβ(1-42), demonstrated similar kinetics of aggregation from the LEDIF peak area. In addition, Figure 1.B shows the average R_h obtained for the 100 µM samples by integration of the LEDIF elution profiles as described elsewhere[21]. At t_{ag} = 0 h and during the first hour of incubation the average R_h was around 1.9 nm (corresponding to the size of the Aβ(1-42) monomer and small oligomer population, in good agreement with previously published works[13, 18]). After about 1 h, the R_h value decreased to reach a plateau around 0.8 nm, which most likely corresponds to the free fluorescent tag or free tagged aminoacids (FITC, theoretical R_h obtained from modelization[13] using HydroPro software[22] on a energy minimized 3D structure is 0.64 nm). In the case of the low concentration samples, the R_h at t_{ag} = 0 h was of 1.95 and 1.85 nm for the 1 µM and the 10 µM samples respectively. The average R_h value decreased very slowly with the appearance of the small sized population (R_h ~ 0.8 nm) and reached the plateau after two weeks for the 1 µM sample (see supporting information figure SI.9). Eventhough it is theoretically

possible to follow the aggregation process at these two low concentrations and for a relatively long period of time, it is not possible to do a control run without the fluorescent tag at these concentrations because of the low sensitivity of the UV detection as compared to fluorescence. Therefore in order to study the impact of the fluorescent tag it seems important to apply conditions were both native and tagged peptides could be followed simultaneously.

In conclusion of this first part, it was found that a high concentration of typically 100 μM was recommended to study the impact of the fluorescent tag on the aggregation process within a reasonnable time range (few days instead of weeks). Therefore, if fluorescent detection combined with a low peptide concentration (below 1 μM) seems hardly applicable for monitoring amyloid peptide aggregation because of slow kinetics, the impact of the fluorescent tag on the aggregation process may however be studied on mixed mixtures of native and tagged peptides, at 100 μM total peptide concentration. To increase the aggregation kinetics for low concentration samples, the use of preformed seeds might also be a suitable option.

3.2. Monitoring the aggregation process of Aβ peptides by TDA-UV

In this work, we used a proportion of tagged peptide between 7 and 10% (see pie charts in Figure 2), keeping constant the total peptide concentration at ~100 μM. Simultaneous UV and fluorescent detections could be compared using these mixed non-tagged and tagged mixtures. The UV detection was used to determine the kinetics of aggregation which can be compared in presence or in absence of tagged peptide. In a recent work[13], we showed by TDA that the products of Aβ peptide aggregation could be divided into four main populations differing by their size. The first population is that of monomeric and small oligomeric forms of the peptides having an $R_h < 5$ nm. The second population corresponds to higher molar mass oligomers with R_h between 4 and 50 nm. The third population shows $R_h > 50$ nm and corresponds to soluble protofibrillar structures. Finally the fourth one is that of insoluble fibrils which size is not accessible by TDA. Figure 3 displays one example of taylorgram deconvolution with the contributions of the different populations to the total UV signal. The residual trace shown in the upper part of Figure 3 (difference between the experimental data and the theoretical fit) represents the soluble fibril fraction.

In Figure 2 are presented the area of the monomer and small oligomers population obtained by deconvolution of the elution profile by UV detection over the whole aggregation process for all the studied systems. The evolution of this population was found to be representative of the

aggregation kinetics[13, 18] via the consumption of the monomeric units. As can be seen from Figure 2A, nAβ(1-40) showed a lag phase of about 18 h before a rapid decrease in the monomeric population to reach a final lower plateau after ~26 h. Aβ(1-40) is thought to follow a secondary nucleation mechanism, where monomers add to already existing fibrils to produce larger fibrils, without going through intermediate states as discussed in the literature[20, 23, 24]. Conversely, the nAβ(1-42) (Figure 2C) decreased rapidly (less than 1h) without showing any lag phase. The 3:1 nAβ(1-40):nAβ(1-42) mixture showed a similar trend as for the nAβ(1-42) sample but with slower kinetics (the plateau was reached after 16 h). As displayed in Figure2D, the addition of 7% of tAβ(1-40) to nAβ(1-40) did not seem to affect the lag phase, however it affected the kinetics of the monomer consumption which reached a plateau after ~60 h instead of 26 h for the 100 % native sample. This observation suggests that the tagged peptide influenced the elongation phase of the aggregation mechanism but not the nucleation step. When the tAβ(1-42) (10%) was added to the nAβ(1-42) sample (see Figure 2G), the kinetics of the aggregation decreased as well and the time to reach the final lower plateau changed from less than 1 h to about 3 h. Similarly, in the case of the 3:1 mixture of Aβ(1-40):Aβ(1-42), when 7% of tagged Aβ(1-40) were added to the sample, the aggregation pathway was not significantly changed compared to the native mixture. However slower kinetics were observed (lower plateau reached after 36 h instead of 16 h for the native mixture; see Figure 2E compared to Figure 2B). These results suggest that the nAβ(1-42) peptide is driving the aggregation process: it rapidly formed the nucleus (no lag phase) and the elongation step was slown by the tAβ(1-40). Likewise, when a fraction of tAβ(1-42) was added to the mixture the aggregation mechanism resembled to the aggregation mechanism of Aβ(1-40) solutions, *i.e.* a lag phase was observed up to about 30 h and then the monomer population proportion decreased until it reached a final plateau at about 60 h. These observations confirmed that the tAβ(1-42) delayed the formation of the Aβ(1-42) nucleus serving as a seed for the elongation of Aβ(1-40). In a study by Zheng *et al.*[9], the effect of several fluorescent tags, among which FITC tag used in this work, on the aggregation process of tAβ(1-42) was investigated using fluorescence correlation spectroscopy. The authors concluded that the FITC tag decreased the propensity of oligomers to aggregate and they attributed this effect to the increase of the peptide hydrophilicity by the fluorescent tag. Further, it was reported that the native Aß(1-42) monomer and its fibrillary structures adopt compacted conformations[25], in which the *N*-terminus is supposedly water-shielded. In this work, the FITC tag can change in the hydrophilic-hydrophobic balance of the peptides, can induce steric hindrance or may change the peptide conformation, leading to a lower propensity for aggregation. For instance, it was reported in

the literature that the *N*-terminally truncated amyloid peptides were more prone to aggregation than the full length ones [26-29] because the truncated peptides would become more hydrophobic, which supports that an increase in hydrohilicity at the *N*-terminus region would impair the aggregation.

Figure 4 shows the hydrodynamic radii obtained for all studied samples and for all populations obtained by deconvolution of the UV elution profile. The monomers and low molar mass oligomers have an R_h of 1.60 – 2.25 nm which was relatively constant during the whole aggregation process (Figure 4, monomers). According to our previous study, these values suggest that this population is mainly comprised of monomers and dimers[13]. As for the higher mass oligomer population, it varied from ~4 to ~30 nm for all studied samples with an average value around 10 nm. Then the R_h of protofibrils ranged from 50 to 250 nm for all studied systems. These results suggest that the fluorescent tag did not influence the size of the different populations when compared to native samples.

When a deeper look is taken at the higher mass oligomer population for the 3:1 mixtures with and without tagged peptides (Figure 5), the following observations could me made: first, in the native peptides mixture, this population increased in proportion and reached a maximum value after 6h incubation and then decreased and reached a lower plateau after 15 h. Then, the addition of tAβ(1-40) did not seem to significantly influence the evolution of this population, which seemed to disappear after 24 h in both cases (with and without tAβ(1-40)). Finally, when tAβ(1-42) was added to the mixture, the bell shaped distribution extended from 0 h up till 60 h with a maximum reached around 30 h, suggesting that the oligomers are more stabilized under these conditions.

The comparison of the evolution of the monomer and small oligomer populations obtained from the elution profiles from the UV and the LEDIF detections (Figure 6), showed no difference in the pathway between the tagged peptide (selectively detected by LEDIF) and the total peptides (detected by UV; composed of tagged and non-tagged peptides), suggesting that the aggregation involves all the different peptides at all steps and that the formed assemblies might be heteromolecular (mixture of Aβ(1-40) and Aβ(1-42)). Figure 6C helps supporting this claim since a rapid decrease of tAβ(1-42) is observed during the first hours of incubation, probably corresponding to the formation of a nucleus, followed by a plateau. Then, another

decrease in the tAβ(1-42) fraction is observed after about 24 h suggesting the onset of the elongation phase with the participation of the Aβ(1-40) (predominantly present in the sample) where the decrease of the monomer population in UV is observed as well.

4. Conclusion

In this work, we showed the ability of TDA to follow the aggregation process of labelled Aβ peptides by fluorescence detection and to study the effect of the label on the aggregation propensity of amyloid peptides. It was found that at very low concentrations (lower than 10 µM) the aggregation kinetics were drastically decreased and the monitoring of the aggregation at these concentrations would be a long process (days or weeks). To increase the kinetics and the experimental throughput, the concentration was increased up to 100 µM with a certain proportion of fluorescent-tagged peptides. At this concentration, it was possible to monitor the aggregation process of Aβ peptide mixtures in a reasonable amount of time. Further, it was reported that the aggregation of Aβ(1-40) and Aβ(1-42) was affected by a small proportion of FITC label. The effect of the fluorescent tag was observed on the elongation phase rather than on the nucleation one. Further, in the case of Aβ(1-40):Aβ(1-42) mixtures, when the tagged peptide was Aβ(1-42), it was observed a higher influence of the FITC label on the aggregation mechanism than with the tagged Aβ(1-40). As a consequence, the formed oligomers in Aβ(1-40):Aβ(1-42) mixtures (with a proportion of tAβ(1-42)) had a substantial increase of their lifetime and potentially of their toxicity. Finally, the comparison of both detection modes allowed to assume that the aggregation mechanism was a heteromolecular process involving both peptide isoforms and both tagged and untagged peptides in the aggregates. In perspective, the study of seeding at low Aβ concentrations and the effect of the truncation on the aggregation process, monitored and speciated by TDA would be an important input into the huge amount of literature dealing with the aggregation of amyloïd peptides.

Data availability statement: “The data that support the findings of this study are available from the corresponding author upon reasonable request.”

Acknowledgments: The authors wish to thank Pr. Luca Cipelletti (L2C Montpellier) for the valuable discussions that helped shape this work.

5. References

1. Selkoe DJ, Hardy J. The amyloid hypothesis of Alzheimer's disease at 25 years. EMBO Mol Med. 2016;8(6):595-608.
2. Lambert MP, Barlow AK, Chromy BA, Edwards C, Freed R, Liosatos M, Morgan TE, Rozovsky I, Trommer B, Viola KL, Wals P, Zhang C, Finch CE, Krafft GA, Klein WL. Diffusible, nonfibrillar ligands derived from $A\beta_{1-42}$ are potent central nervous system neurotoxins. Proc Natl Acad Sci U S A. 1998;95(11):6448-53.
3. Hardy JA, Higgins GA. Alzheimer's disease: the amyloid cascade hypothesis. Science. 1992;256(5054):184-5.
4. Lazarevic V, Fieńko S, Andres-Alonso M, Anni D, Ivanova D, Montenegro-Venegas C, Gundelfinger ED, Cousin MA, Fejtova A. Physiological Concentrations of Amyloid Beta Regulate Recycling of Synaptic Vesicles via Alpha7 Acetylcholine Receptor and CDK5/Calcineurin Signaling. Front Mol Neurosci. 2017;10.
5. Rice LJ, Ecroyd H, van Oijen AM. Illuminating amyloid fibrils: Fluorescence-based single-molecule approaches. Computational and Structural Biotechnology Journal. 2021;19:4711-24.
6. Wägele J, De Sio S, Voigt B, Balbach J, Ott M. How Fluorescent Tags Modify Oligomer Size Distributions of the Alzheimer Peptide. Biophys J. 2019;116(2):227-38.
7. Quinn SD, Dalgarno PA, Cameron RT, Hedley GJ, Hacker C, Lucocq JM, Baillie GS, Samuel IDW, Penedo JC. Real-time probing of β-amyloid self-assembly and inhibition using fluorescence self-quenching between neighbouring dyes. Mol Biosyst. 2014;10(1):34-44.
8. Taverna M, Crosnier de Lassichère C, Mai TD, Otto M, inventors; Méthode de stabilisation d'un peptide. France patent FR3095520A1. 2019.
9. Zheng Y, Xu L, Yang J, Peng X, Wang H, Yu N, Hua Y, Zhao J, He J, Hong T. The effects of fluorescent labels on Aβ42 aggregation detected by fluorescence correlation spectroscopy. Biopolymers. 2018;109(11):e23237.
10. Hu X, Crick SL, Bu G, Frieden C, Pappu RV, Lee J-M. Amyloid seeds formed by cellular uptake, concentration, and aggregation of the amyloid-beta peptide. Proc Natl Acad Sci U S A. 2009;106(48):20324-9.
11. Sowade RF, Jahn TR. Seed-induced acceleration of amyloid-β mediated neurotoxicity in vivo. Nature Communications. 2017;8(1):512.
12. Wang L, Eom K, Kwon T. Different Aggregation Pathways and Structures for Aβ40 and Aβ42 Peptides. Biomolecules. 2021;11(2).
13. Deleanu M, Hernandez JF, Cipelletti L, Biron JP, Rossi E, Taverna M, Cottet H, Chamieh J. Unraveling the Speciation of beta-Amyloid Peptides during the Aggregation Process by Taylor Dispersion Analysis. Anal Chem. 2021;93(16):6523-33.
14. Roher AE, Lowenson JD, Clarke S, Woods AS, Cotter RJ, Gowing E, Ball MJ. beta-Amyloid-(1-42) is a major component of cerebrovascular amyloid deposits: implications for the pathology of Alzheimer disease. Proc Natl Acad Sci U S A. 1993;90(22):10836-40.
15. Jan A, Gokce O, Luthi-Carter R, Lashuel HA. The ratio of monomeric to aggregated forms of Abeta40 and Abeta42 is an important determinant of amyloid-beta aggregation, fibrillogenesis, and toxicity. J Biol Chem. 2008;283(42):28176-89.
16. Cukalevski R, Yang X, Meisl G, Weininger U, Bernfur K, Frohm B, Knowles TPJ, Linse S. The Aβ40 and Aβ42 peptides self-assemble into separate homomolecular fibrils in binary mixtures but cross-react during primary nucleation. Chemical Science. 2015;6(7):4215-33.
17. Cerofolini L, Ravera E, Bologna S, Wiglenda T, Böddrich A, Purfürst B, Benilova I, Korsak M, Gallo G, Rizzo D, Gonnelli L, Fragai M, De Strooper B, Wanker EE, Luchinat C. Mixing Aβ(1–40) and Aβ(1–42) peptides generates unique amyloid fibrils. Chem Commun. 2020;56(62):8830-3.
18. Deleanu M, Deschaume O, Cipelletti L, Hernandez J-F, Bartic C, Cottet H, Chamieh J. Taylor Dispersion Analysis and Atomic Force Microscopy Provide a Quantitative Insight into the Aggregation Kinetics of Aβ (1–40)/Aβ (1–42) Amyloid Peptide Mixtures. ACS Chem Neurosci. 2022;13(6):786-95.
19. Brinet D, Kaffy J, Oukacine F, Glumm S, Ongeri S, Taverna M. An improved capillary electrophoresis method for in vitro monitoring of the challenging early steps of Aβ(1-42) peptide oligomerization: Application to anti-Alzheimer's drug discovery. Electrophoresis. 2014;35(23):3302-9.

20. Lattanzi V, Bernfur K, Sparr E, Olsson U, Linse S. Solubility of Aβ40 peptide. JCIS Open. 2021;4:100024.
21. Chamieh J, Cottet H. Comparison of single and double detection points Taylor Dispersion Analysis for monodisperse and polydisperse samples. J Chromatogr A. 2012;1241:123-7.
22. Ortega A, Amorós D, García de la Torre J. Prediction of Hydrodynamic and Other Solution Properties of Rigid Proteins from Atomic- and Residue-Level Models. Biophys J. 2011;101(4):892-8.
23. Arosio P, Knowles TPJ, Linse S. On the lag phase in amyloid fibril formation. PCCP. 2015;17(12):7606-18.
24. Chen Y-R, Glabe CG. Distinct Early Folding and Aggregation Properties of Alzheimer Amyloid-β Peptides Aβ40 and Aβ42. J Biol Chem. 2006;281(34):24414-22.
25. Barz B, Buell AK, Nath S. Compact fibril-like structure of amyloid β-peptide (1–42) monomers. Chem Commun. 2021;57(7):947-50.
26. Dunys J, Valverde A, Checler F. Are N- and C-terminally truncated Aβ species key pathological triggers in Alzheimer's disease? J Biol Chem. 2018;293(40):15419-28.
27. Bouter Y, Dietrich K, Wittnam JL, Rezaei-Ghaleh N, Pillot T, Papot-Couturier S, Lefebvre T, Sprenger F, Wirths O, Zweckstetter M, Bayer TA. N-truncated amyloid β (Aβ) 4-42 forms stable aggregates and induces acute and long-lasting behavioral deficits. Acta Neuropathol. 2013;126(2):189-205.
28. Rostagno A, Cabrera E, Lashley T, Ghiso J. N-terminally truncated Aβ4-x proteoforms and their relevance for Alzheimer's pathophysiology. Translational Neurodegeneration. 2022;11(1):30.
29. Bayer TA. N-Truncated Aβ Starting at Position Four—Biochemical Features, Preclinical Models, and Potential as Drug Target in Alzheimer's Disease. Front Aging Neurosci. 2021;13.

Figure Captions

Figure 1. (A) Evolution of the peak area (normalized with the peak area at t_{ag} = 0 h) obtained by integration of the elution profiles with the LEDIF detection for all analyzed incubation times for 100 % tAβ(1-42) solutions at 1 µM (squares), 10 µM (circles) and 100 µM (triangles), and for a 100 µM Aβ(1-42) solution constituted of 90% nAβ(1-42) and 10% tAβ(1-42) (inversed triangles). (B) Comparison of the average hydrodynamic radii (obtained by integrating the LEDIF elution profile as described in[21]) over the whole aggregation study for the 100 µM Aβ(1-42) solutions (100 % tAβ(1-42) (triangles) and the mixture of 90% nAβ(1-42) and 10% tAβ(1-42) (inversed triangles)).

Figure 2. Peak area evolution of the monomer and small oligomer populations obtained for both nAβ + tAβ systems and 100 % nAβ experiments at 100 µM total peptide concentration (except for 3:1 native peptides mixture where the concentration was of 133 µM) as obtained from the analysis of the UV-TDA elution profile: (A) 100% nAβ(1-40), (B) 75% nAβ(1-40) + 25% nAβ(1-42), (C) 100% nAβ(1-42), (D) 93% nAβ(1-40) + 7% tAβ(1-40), (E) 68% nAβ(1-40) + 7% nAβ(1-40) + 25% nAβ(1-42), (F) 75% nAβ(1-40) + 15% nAβ(1-42) + 10% tAβ(1-42) and (G) 90% nAβ(1-42) + 10% tAβ(1-42). Peak area was normalized to obtain a better comparison of the species evolution, by dividing the area of each data point to the total peak area obtained for the first run at t_{ag} = 0 h. The inserted pie charts denote the proportion of the nAβ and tAβ content in the studied samples.

Figure 3: Example of data processing of the experimental taylorgrams. The lower graph represents the experimental data (black) fitted with the sum of four Gaussian peaks (dashed orange) which are individually represented on the graph. The residuals plot in the upper part of the graphs is the difference between the experimental data and the theoretical fit. Experimental conditions: Sample: 100 µM of 3:1 Aβ(1-40):Aβ(1-42) mixture (68% nAβ(1-40) + 7% tAβ(1-40) + 25 % nAβ(1-42)) at t_{ag} = 16 h; 20 mM phosphate buffer pH 7.4. Incubation: quiescent conditions at 37 °C. Fused silica capillaries: 50 µm i.d. × 60 cm × 51.5 cm. Mobile phase: 20 mM phosphate buffer, pH 7.4. Mobilization pressure: 100 mbar. Injection: 44 mbar for 4 s. Analyses were performed at 37 °C. UV detection at 191 nm. Baseline treatment was performed in Microcal Origin. The experimental fitting of the taylorgrams was performed by using the sum of four Gaussian functions in Microsoft Excel.

Figure 4. Hydrodynamic radius evolution of the species obtained for both nAβ + tAβ systems and 100 % nAβ experiments during the UV analysis: (A) 100% nAβ(1-40), (B) 3:1 Aβ(1-40):Aβ(1-42) - 75% nAβ(1-40) + 25% nAβ(1-42), (C) 100% nAβ(1-42), (D) 93% nAβ(1-40) + 7% tAβ(1-40), (E) 3:1 Aβ(1-40):Aβ(1-42) - 68% nAβ(1-40) + 7% tAβ(1-40) + 25 % nAβ(1-42), (F) 3:1 Aβ(1-40):Aβ(1-42) - 75% nAβ(1-40) + 15% nAβ(1-42) + 10% tAβ(1-42), (G) 90% nAβ(1-42) + 10% tAβ(1-42). The species are represented as follows: monomer and low molar mass oligomers (squares, ■), higher molar mass oligomers (circles, ●) and protofibrils (triangles, ▲). Experimental conditions: Sample: 100 µM total Aβ; 20 mM phosphate buffer, pH 7.4. Incubation: quiescent conditions at 37 °C. Fused silica capillaries: 50 µm i.d. × 60 cm × 51.5 cm. Mobile phase: 20 mM phosphate buffer, pH 7.4. Mobilization pressure: 100 mbar. Injection: 44 mbar for 4 s, $V_i \approx 7$ nL ($V_i/V_d \approx 0.6$ %). Analyses were performed at 37 °C. UV detection at 191 nm.

Figure 5. Peak area evolution of the higher molar mass oligomer population obtained from the UV analysis of the TDA elution profile for 3:1 Aβ(1-40):Aβ(1-42) - 75% nAβ(1-40) + 25% nAβ(1-42) (squares); 3:1 Aβ(1-40):Aβ(1-42) - 68% nAβ(1-40) + 7% nAβ(1-40) + 25% nAβ(1-42) (circles); and 3:1 Aβ(1-40):Aβ(1-42) - 75% nAβ(1-40) + 15% nAβ(1-42) + 10% tAβ(1-42) (triangles). Peak area was normalized, to obtain a better comparison of the species evolution, by dividing the area of each data point to the total peak area obtained for the first run at t_{ag} = 0 h.

Figure 6. Comparison of the peak area evolution of the monomer and small oligomer populations obtained by UV detection (closed symbols) and LEDIF detection (open symbols) for nAβ + tAβ systems: (A) 93% nAβ(1-40) + 7% tAβ(1-40), (B) 3:1 Aβ(1-40):Aβ(1-42) - 68% nAβ(1-40) + 7% nAβ(1-40) + 25% nAβ(1-42), (C) 3:1 Aβ(1-40):Aβ(1-42) - 75% nAβ(1-40) + 15% nAβ(1-42) + 10% tAβ(1-42) and (D) 90% nAβ(1-42) + 10% tAβ(1-42). Peak area was normalized to obtain a better comparison of the species evolution by dividing the area of each data point to the total peak area obtained for the first run at t_{ag} = 0 h. The inserted pie charts denote the proportion of the nAβ and tAβ content in the studied samples.

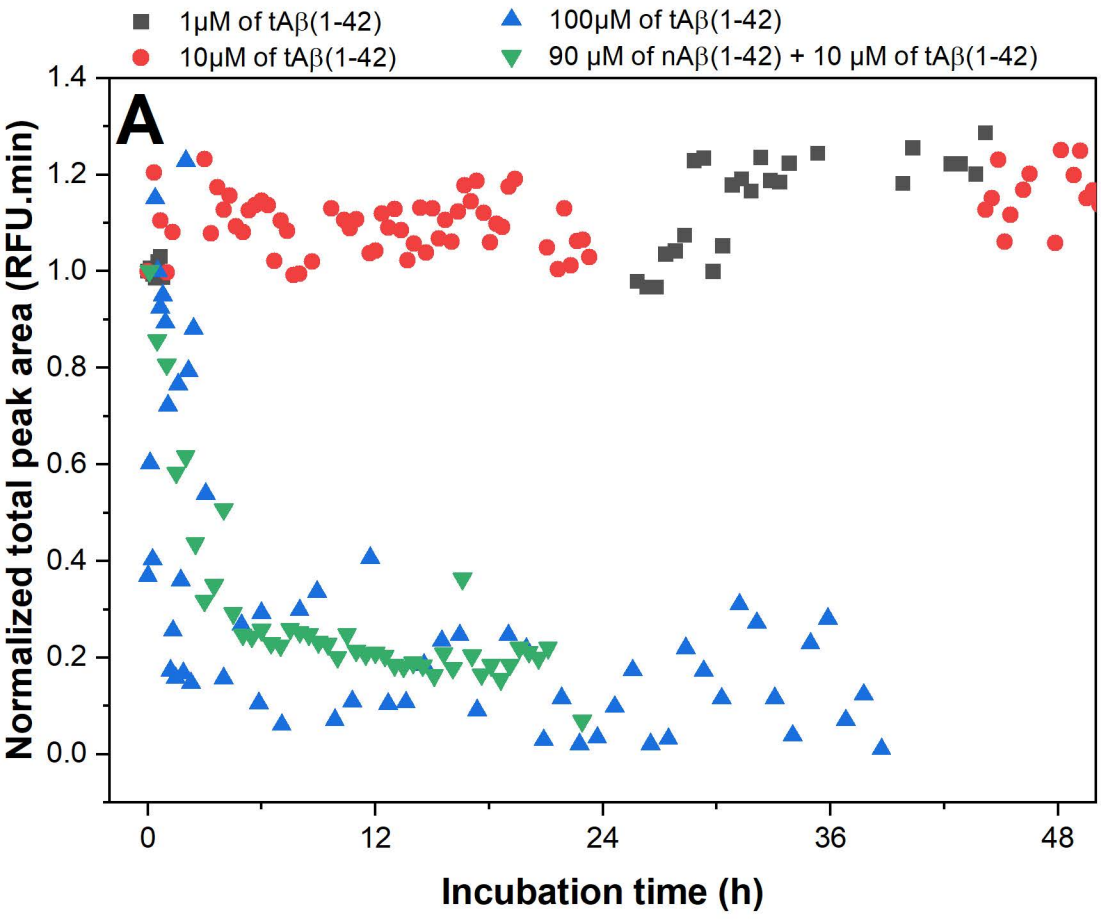
1μM of tAβ(1-42)
10μM of tAβ(1-42)
100μM of tAβ(1-42)
90 μM of nAβ(1-42) + 10 μM of tAβ(1-42)
A
Normalized total peak area (RFU.min)
Incubation time (h)

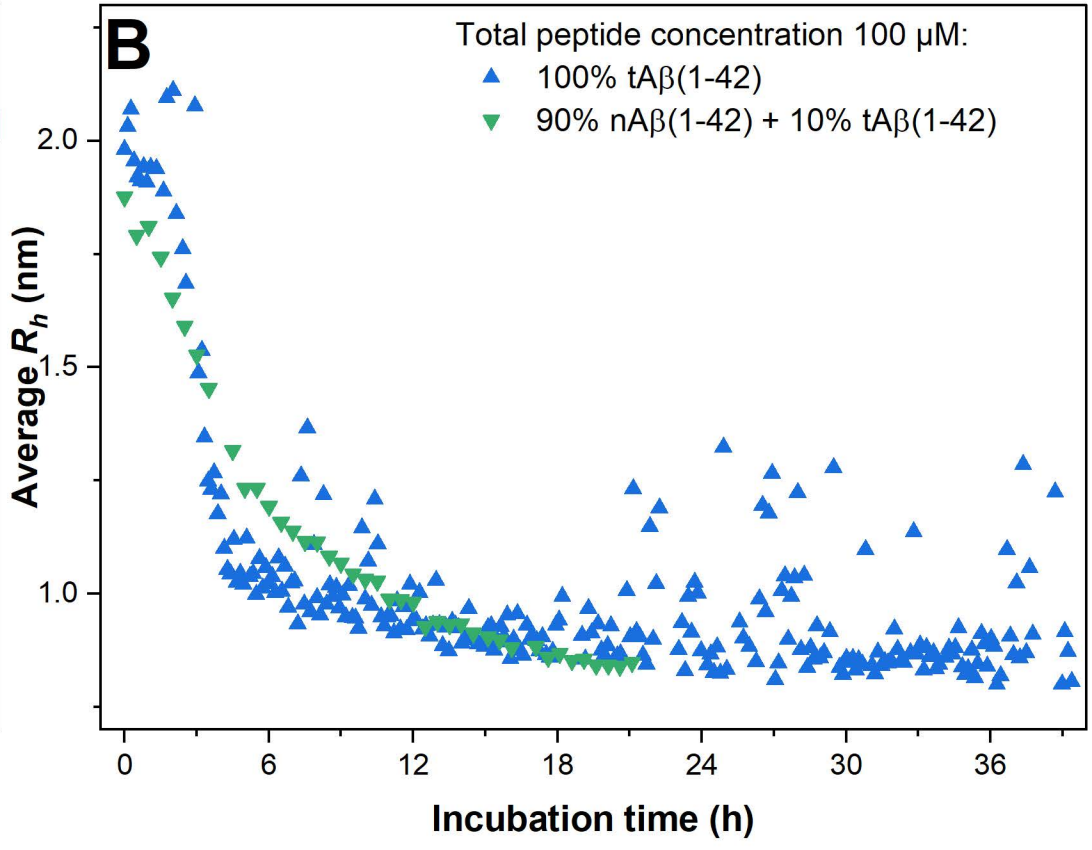
B
Total peptide concentration 100 μM:
100% tAβ(1-42)
90% nAβ(1-42) + 10% tAβ(1-42)
Average R_h (nm)
Incubation time (h)

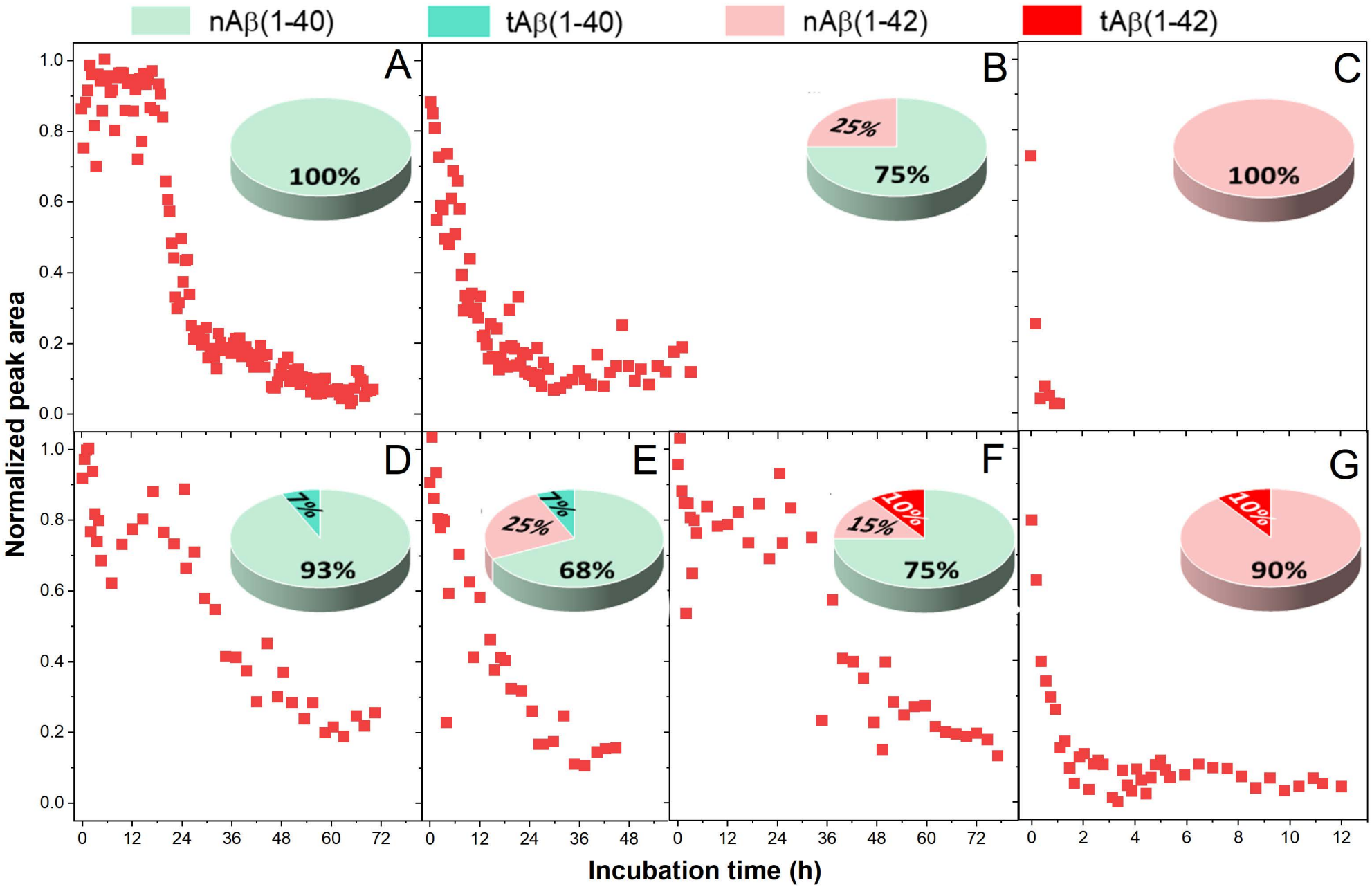
nAβ(1-40)
tAβ(1-40)
nAβ(1-42)
tAβ(1-42)
A
B
C
D
E
F
G
100%
25%
75%
100%
7%
93%
7%
25%
68%
10%
15%
75%
10%
90%
Normalized peak area
Incubation time (h)

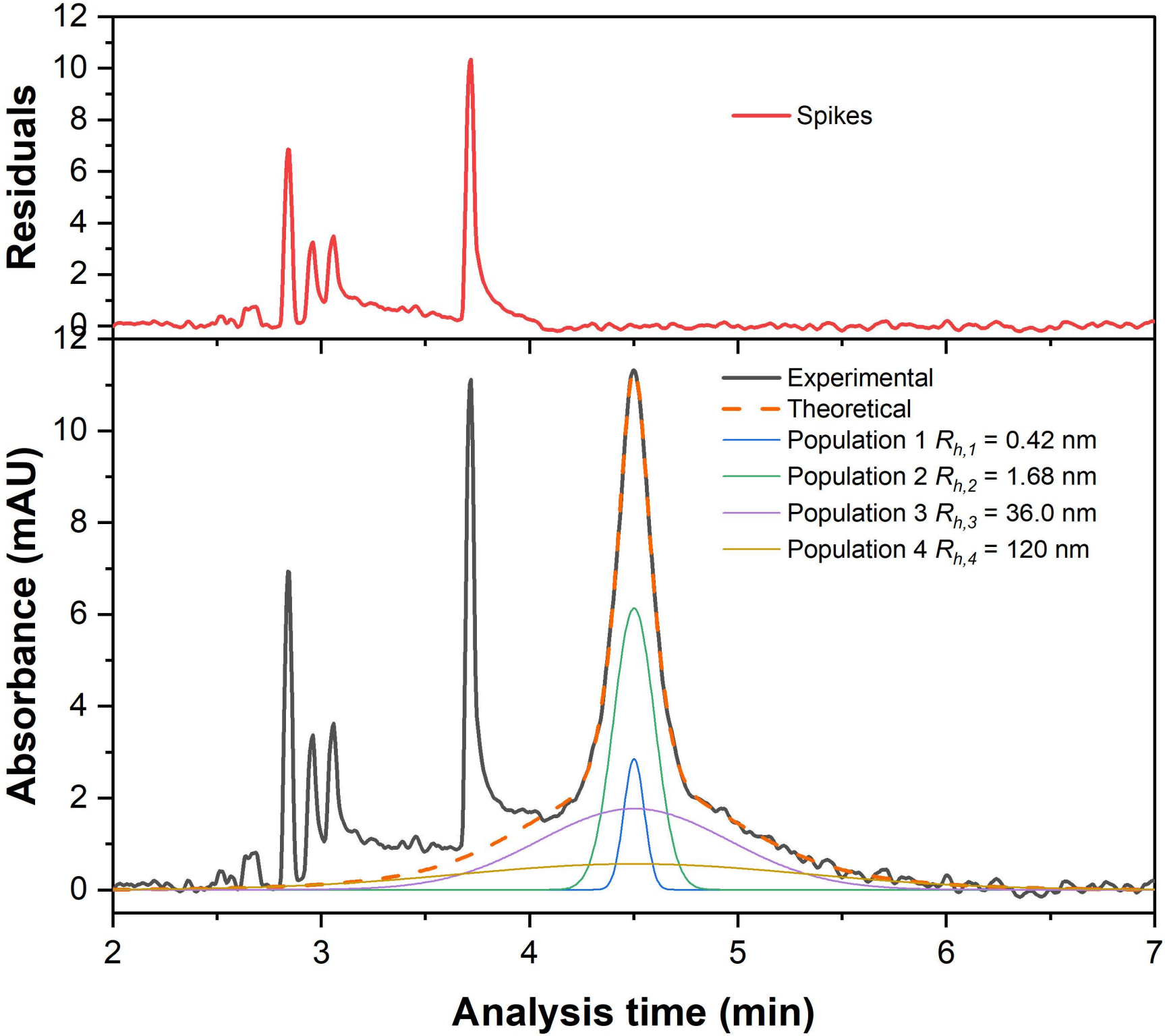
Residuals
Spikes
Absorbance (mAU)
Experimental
Theoretical
Population 1 $R_{h,1}$ = 0.42 nm
Population 2 $R_{h,2}$ = 1.68 nm
Population 3 $R_{h,3}$ = 36.0 nm
Population 4 $R_{h,4}$ = 120 nm
Analysis time (min)

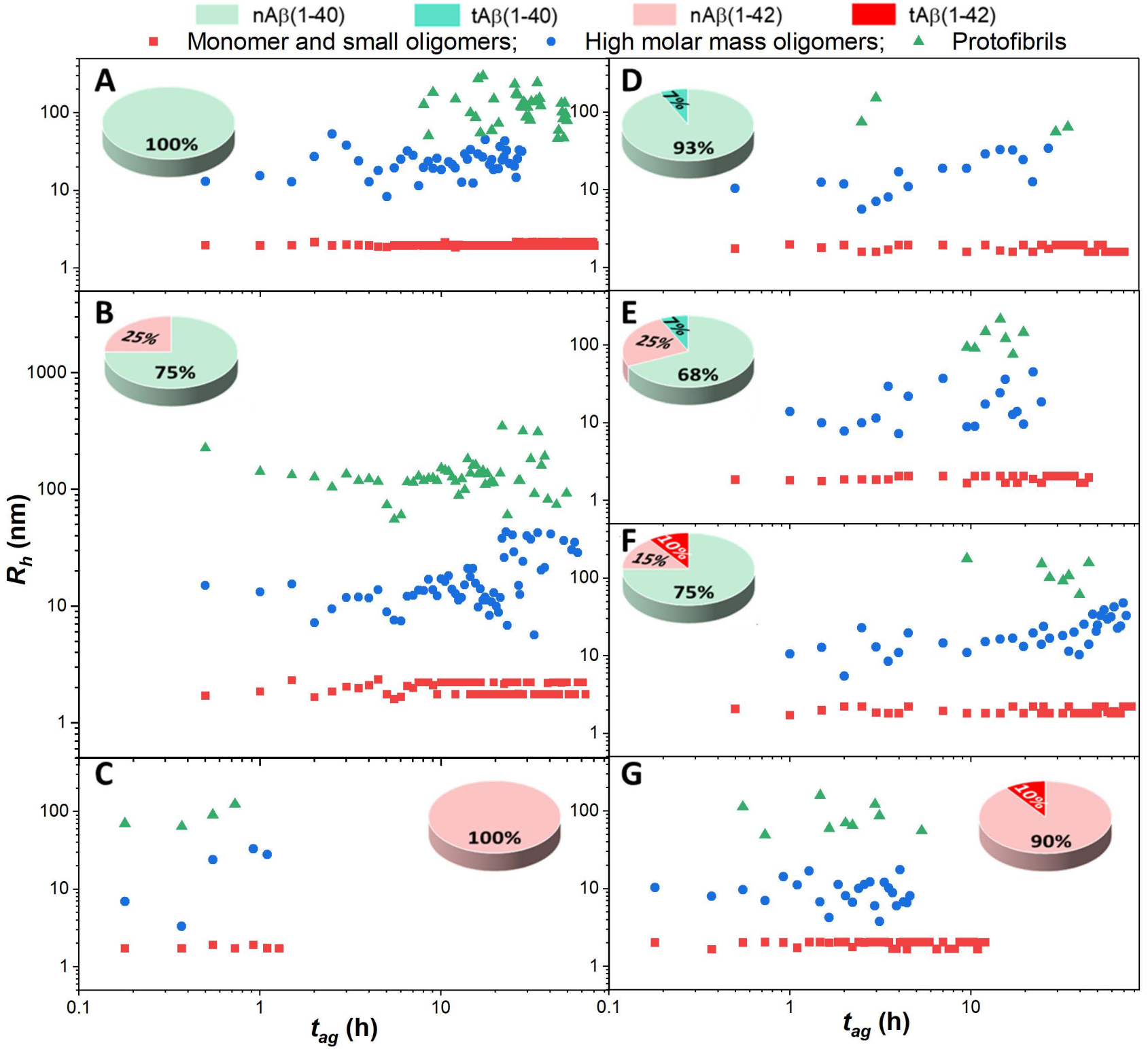
nAβ(1-40)
tAβ(1-40)
nAβ(1-42)
tAβ(1-42)
Monomer and small oligomers;
High molar mass oligomers;
Protofibrils
A
100%
B
25%
75%
C
100%
D
7%
93%
E
7%
25%
68%
F
10%
15%
75%
G
10%
90%
R_h (nm)
t_{ag} (h)
t_{ag} (h)

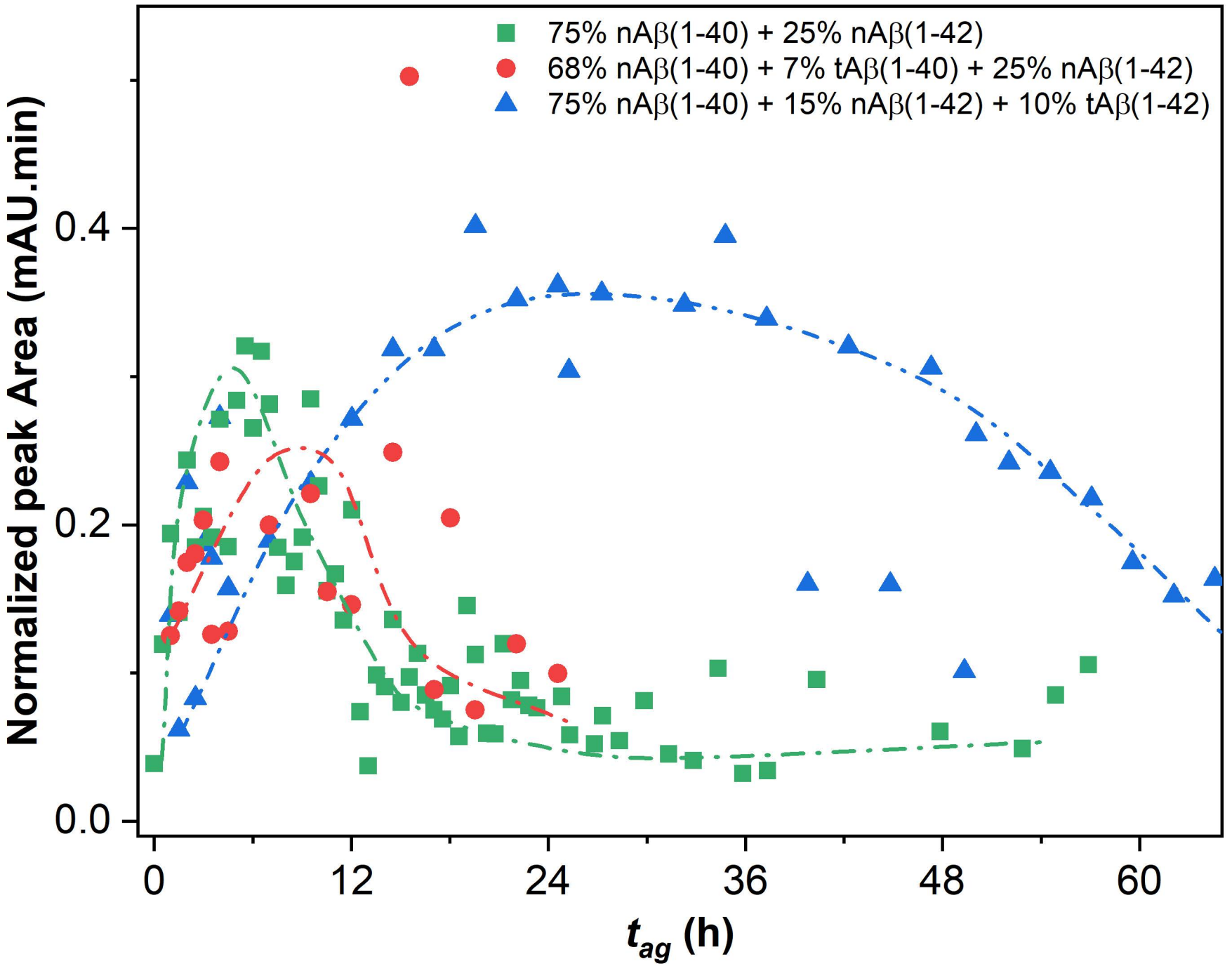
75% nAβ(1-40) + 25% nAβ(1-42)
68% nAβ(1-40) + 7% tAβ(1-40) + 25% nAβ(1-42)
75% nAβ(1-40) + 15% nAβ(1-42) + 10% tAβ(1-42)
Normalized peak Area (mAU.min)
0.0
0.2
0.4
0
12
24
36
48
60
t_{ag} (h)

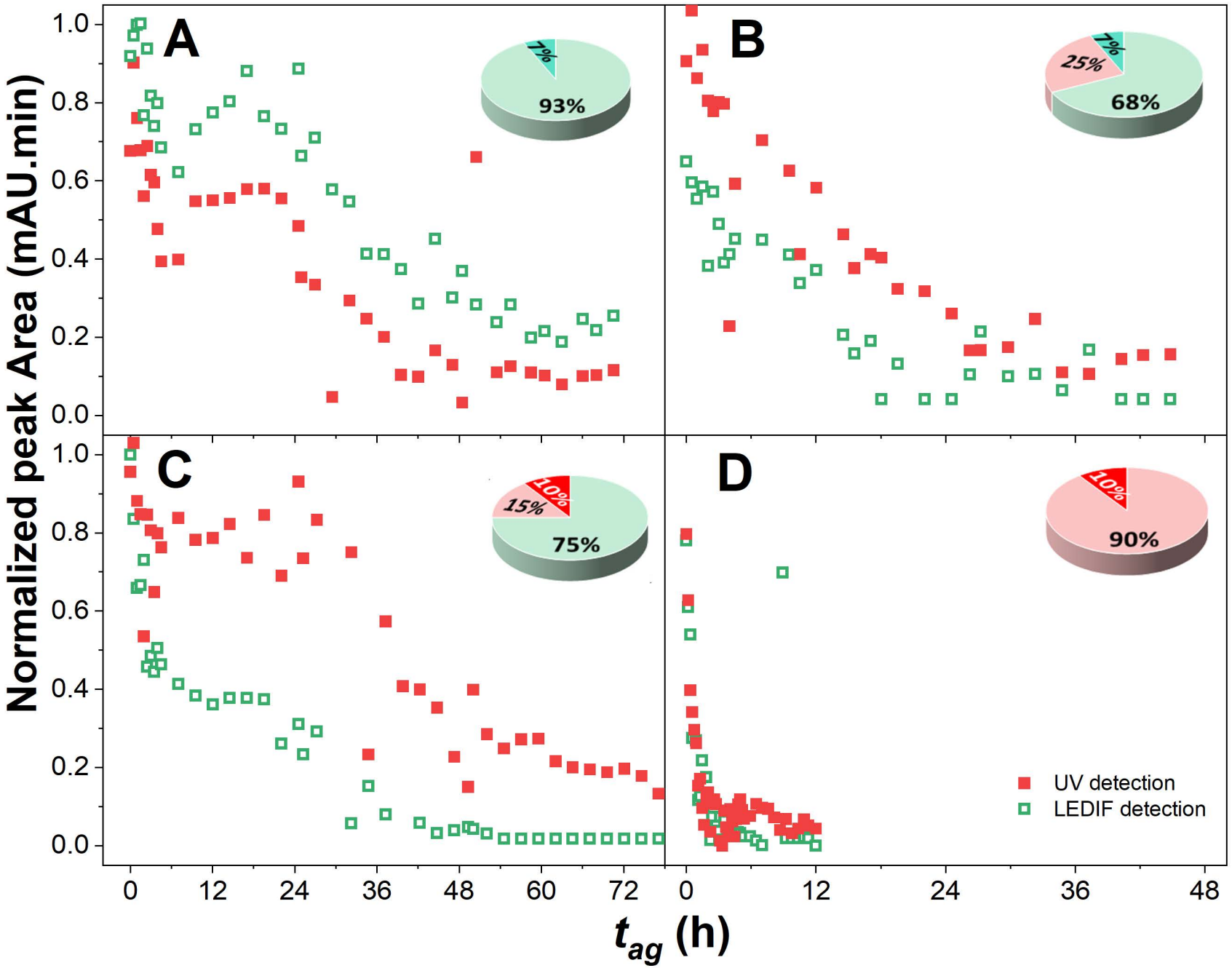
A
B
C
D
7%
93%
7%
25%
68%
10%
15%
75%
10%
90%
UV detection
LEDIF detection
Normalized peak Area (mAU.min)
t_{ag} (h)
0.0
0.2
0.4
0.6
0.8
1.0
0
12
24
36
48
60
72